RSC Advances

PAPER

View Article Online
View Journal | View Issue

Cite this: *RSC Adv.*, 2025, **15**, 17290

Synthesis and characterization of novel *N*-(2-(pyrazin-2-yl-oxy)ethyl)-4-(trifluoromethoxy) benzamide scaffolds, and biological evaluation and molecular docking studies†

Venkata Konda Prasad. B,[ab] G. Venkata Haritha,[c] Kavati Shireesha,[a] Kumara Swamy Jella, *[a] Dharavath Ravi[d] and Ajmeera Ramesh[e]

Received 6th February 2025
Accepted 15th May 2025

DOI: 10.1039/d5ra00879d

rsc.li/rsc-advances

A new series of biologically potent *N*-(2-(6-substituted-1*H*-pyrazin-2-yloxy)ethyl)-4-(trifluoromethoxy) benzamide scaffolds was synthesized, and their structures were confirmed by ^{1}H NMR, ^{13}C NMR, and mass spectrometry. All the synthesized molecules were tested against antibacterial activity against various pathogenic microorganisms and exhibited remarkable activity. Compounds **12a** and **13a** exhibited good antibacterial activity against pathogenic cell lines, *Staphylococcus aureus* and *Escherichia coli*. Additionally, synthesized molecules **12a** and **13a** were screened for anticancer activity against the A549 (lung cancer) cell line. These compounds displayed excellent anticancer activity with IC_{50} values of 19 + 0.50 μM, 17 ± 0.5 μM, A549 (lung cancer). Molecular docking studies results were well supported by strong intercalative interactions of the synthesized compounds with target proteins.

Introduction

Pyrazines are heterocyclic compounds characterized by a six-membered ring with two nitrogen atoms. These compounds serve as versatile scaffolds in medicinal chemistry due to their electronic properties and ability to participate in diverse chemical interactions. Structural modifications of the pyrazine ring allow for fine-tuning of biological activity and specificity. Nitrogen atoms in the ring system facilitate hydrogen bonding and metal coordination, broadening their biological applications.[1–5] Pyrazine derivatives have garnered attention in medicinal chemistry due to their diverse biological activities.[6–9] Recent studies highlight their potential as antimicrobial agents and their promising cytotoxicity against lung cancer cells.[10–12] In recent years, the quest for novel bioactive compounds has driven significant research into diverse chemical classes with potential therapeutic applications. Among these, pyrazine derivatives have emerged as a prominent area of interest due to their versatile biological activities.[13,14] The antimicrobial properties of pyrazine derivatives have garnered particular attention as the global rise in antimicrobial resistance challenges conventional treatment strategies.[15] These derivatives have demonstrated significant efficacy against various pathogenic microorganisms, including bacteria and fungi.[16] Their ability to inhibit microbial growth and potentially overcome resistance mechanisms makes them valuable candidates for developing new antimicrobial agents.[17] Over the years, numerous drugs and bioactive molecules have been developed based on the pyrazine core moiety; among them, some medicinally potent pyrazine drug derivatives are shown in Fig. 1.

In addition to their antimicrobial potential, pyrazine derivatives have also shown promise in oncology. Cancer remains a leading cause of morbidity and mortality worldwide, and the search for effective, targeted therapies is crucial. Pyrazine-based compounds have exhibited cytotoxic effects against various cancer cell lines, including those of lung cancer,[18–23] which is one of the most prevalent and aggressive types of cancer. The ability of these compounds to induce selective toxicity in cancer cells while sparing normal cells is of particular interest in designing more effective and less toxic cancer therapies.

In this manuscript, we explore the synthesis and evaluation of new *N*-(2-(6-substituted1-yl)pyrazin-2-yloxy)ethyl)-4-(trifluoromethoxy)benzamide derivatives, focusing on their antimicrobial activities and cytotoxic effects against human lung cancer cell lines. By investigating these dual properties,

[a]*Department of Chemistry, Chaitanya (Deemed to be University), Ranga Reddy, Hyderabad, Telangana 500075, India. E-mail: jkchem14@gmail.com*

[b]*Syngene International Ltd, Hyderabad, Telangana 500078, India*

[c]*Department of Chemistry, Rayalaseema University, Kurnool, Andhra Pradesh 518007, India*

[d]*Department of Chemistry, Osmania University, Hyderabad 500007, India*

[e]*Department of Chemistry, National Institute of Technology, Warangal 506004, India*

† Electronic supplementary information (ESI) available. See DOI: https://doi.org/10.1039/d5ra00879d

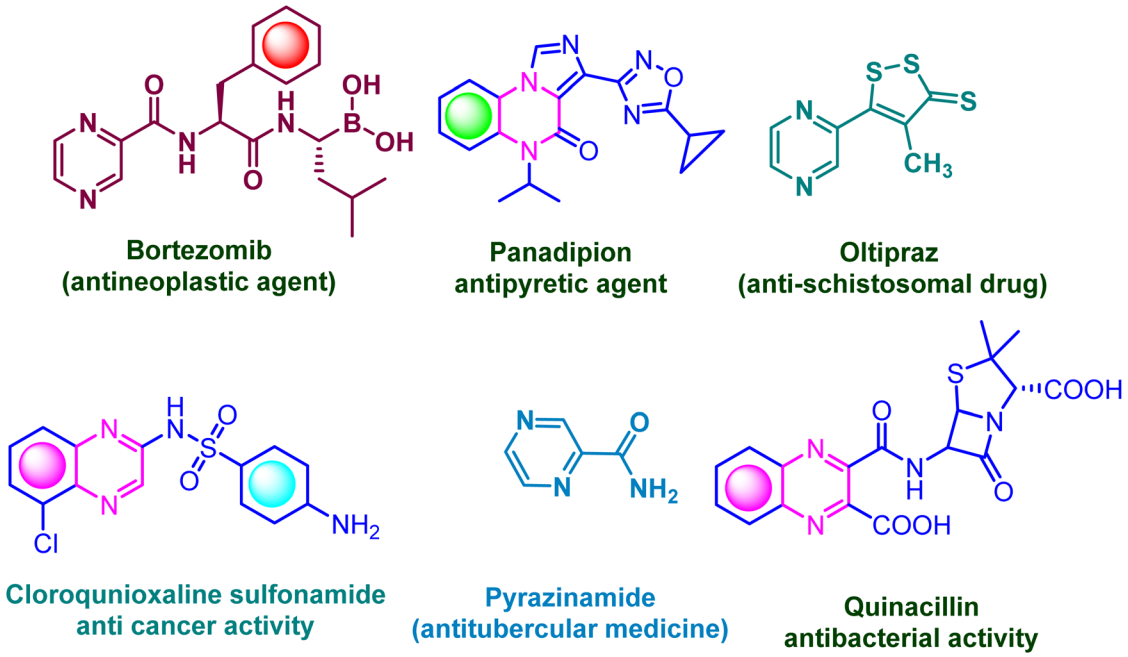

Fig. 1 Chemical structure of biologically potent pyrazine drugs.

we aim to contribute to developing new therapeutic agents that address both infectious diseases and cancer, potentially offering new avenues for treatment in these critical areas. In this manuscript, the present work describes the synthesis of a novel series of *N*-(2-((6-substituted pyrazin-2-yloxy)ethyl)-4-(trifluoromethoxy)benzamide derivatives. These compounds were synthesized using a key intermediate, *N*-(2-((6-chloropyrazin-2-yl)oxy)ethyl)-4-(trifluoromethoxy)benzamide (**5**), which was further derivatized through nucleophilic substitution and palladium-catalyzed cross-coupling reactions.

Results and discussions

The synthetic route of newly prepared compounds (**6a–20a**) was represented in Scheme 1. Initially, the starting material *N*-(2-hydroxyethyl)-4-(trifluoromethoxy)benzamide (**3**) was easily synthesized from 4-(trifluoromethoxy)benzoic acid (**1**) and 2-aminoethanol (**2**), in the presence of *N*,*N*-diisopropylethylamine (DIPEA), 1-hydroxybenzotriazole (HOBt) (1.5 eq.), and *N*,*N*-ethyl carbodiimide hydrochloride (EDC·HCl) (1.5 eq.) was added at 0 °C and stirred for 12 h at 25 °C, furnishing compound **3** with an excellent yield. Then, compound *N*-(2-hydroxyethyl)-4-(trifluoromethoxy)benzamide reacted with 2,6-dichloro pyrazine (**4**) in the presence of potassium *tert*-butoxide (1.1 eq.) in THF (20 mL) at 0 °C and stirred for 2 h at 25 °C obtained reaction intermediate *N*-(2-((6-chloropyrazin-2-yl)oxy)ethyl)-4-(trifluoromethoxy)benzamide (**5**) good yield. In this study, a pyrazine-based intermediate, *N*-(2-((6-chloropyrazin-2-yl)oxy) ethyl)-4-(trifluoromethoxy)benzamide (compound **5**), was employed as a key scaffold for the synthesis of a series of novel target derivatives. The synthesis strategy involved the formation of a new carbon–nitrogen (C–N) bond, enabling the development of *N*-(2-((6-substituted pyrazin-2-yloxy)ethyl)-4-(trifluoromethoxy)benzamide derivatives, labeled as **6a–20a**. For derivatives (**6a–16a**), condensation reactions were carried out between compound **5** and various amine-containing reagents in dimethyl sulfoxide (DMSO) under optimized temperature conditions. This route allowed efficient nucleophilic substitution at the 6-chloropyrazine moiety. In contrast, compounds (**17a–20a**) were synthesized *via* palladium-catalyzed amination reactions. These reactions were conducted in 1,4-dioxane, employing cesium carbonate (Cs_2CO_3) as a base and Brett Phos Pd G3 as the catalyst, under conventional heating conditions. This protocol facilitated the formation of C–N bonds with amines that required more reactive or sterically hindered systems.

All desired compounds were obtained in moderate to high yields, ranging from 53% to 90%, indicating the efficiency and versatility of the developed synthetic methodologies. The structures of the synthesized compounds were unambiguously confirmed using liquid chromatography-mass spectrometry (LC-MS), ^{1}H NMR, and ^{13}C NMR spectroscopic techniques. Detailed yields and structural assignments are summarized in Table 1.

Biological evaluation

Anti-cancer activity

Cell culture. The Human lung cancer (A549)[24–28] cells were procured from the National Center for Cell Sciences (NCCS), Pune, India. The selected cancer cells were maintained in Dulbecco's modified eagles' medium (DMEM) supplemented with 2 mM l-glutamine and balanced salt solution (BSS) adjusted to

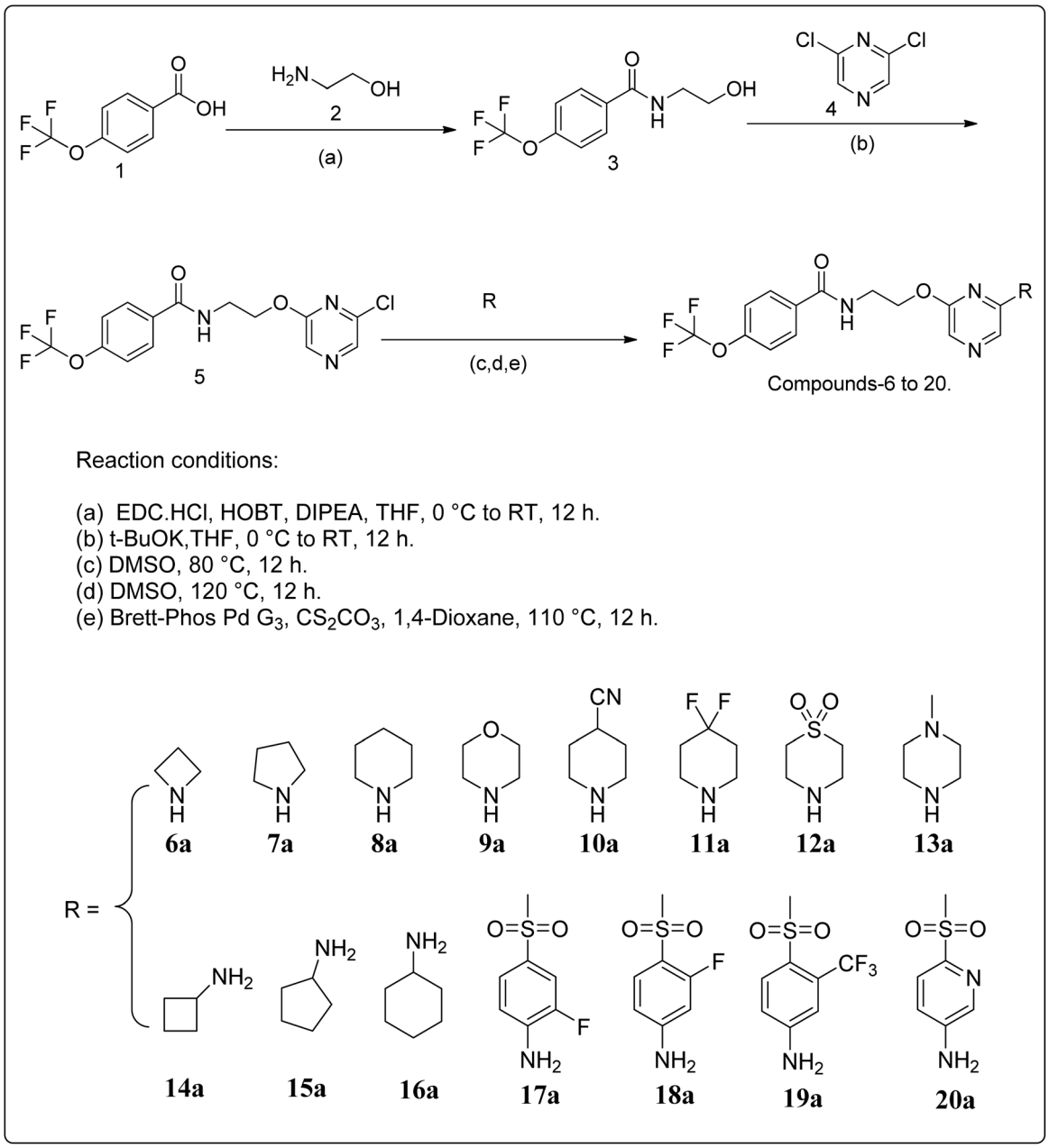

Scheme 1 Synthesis of substituted novel *N*-(2-(pyrazin-2-yl-oxy)ethyl)-4-(trifluoromethoxy)benzamide scaffolds derivatives (**6a–20a**).

contain 1.5 g L^{-1} Na_2CO_3, 0.1 mM non-essential amino acids, 1 mM sodium pyruvate, 2 mM l-glutamine, 1.5 g L^{-1} glucose, 10 mM (4-(2-hydroxyethyl)-1-piperazineethane sulfonic acid) (HEPES) and 10% fetal bovine serum (GIBCO, USA). Penicillin and streptomycin (100 IU/100 μg) were adjusted to 1 mL L^{-1}. The cells were maintained at 37 °C with 5% CO_2 in a humidified CO_2 atmosphere.

Morphological study. The selected cells that were grown on cover slips (1×10^5 cells per cover slip) were incubated with the complex at different concentrations, and they were then fixed in an ethanol: acetic acid solution (3 : 1, v/v). The cover slips were gently mounted on glass slides for the morphometric analysis. Three monolayers per experimental group were micrographed. The morphological changes of the cells were analyzed using Nikon (Japan) bright field inverted light microscopy at 10× magnification.

Evaluation of cytotoxicity

The inhibitory concentration (IC_{50}) value was evaluated using an MTT [3-(4,5-dimethylthiazol-2-yl)-2,5-diphenyltetrazolium bromide] assay. The cells were grown (1×10^4 cells per well) in a 96-well plate for 48 h to 80% confluence. The medium was replaced with fresh medium containing the serially diluted sample, and the cells were further incubated for 48 h. The

Table 1 Synthesis of substituted pyrazine derivatives (**6a–20a**) under the conventional method in the presence of Brett-Phos Pd G_3

S. No.	Comp.	Synthesized final compounds	M. P. (°C)	Yield (%)
1	**6a**	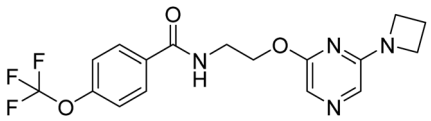	103	63
2	**7a**	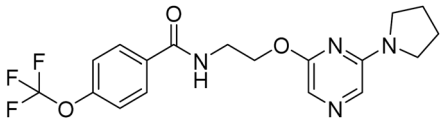	106	86
3	**8a**	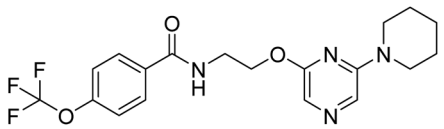	113	90
4	**9a**	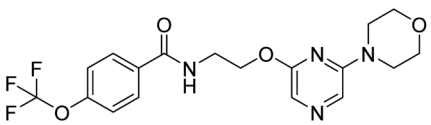	136	87
5	**10a**	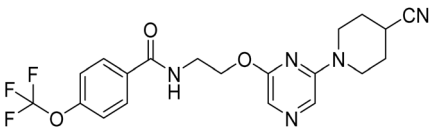	168	56
6	**11a**	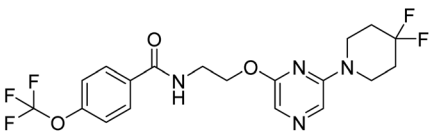	189	62
7	**12a**	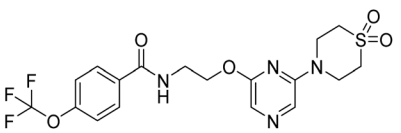	196	63
8	**13a**	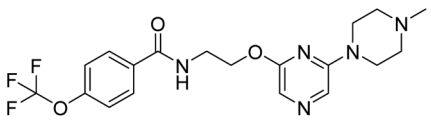	188	89
9	**14a**	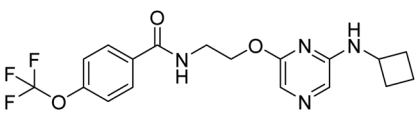	150	58
10	**15a**	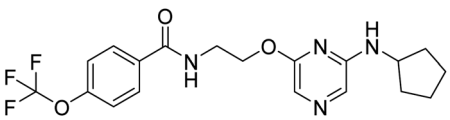	165	66
11	**16a**	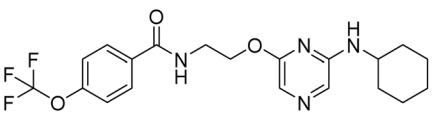	180	55
12	**17a**	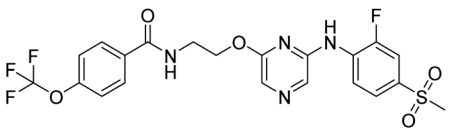	110	64

Table 1 (*Contd.*)

S. No.	Comp.	Synthesized final compounds	M. P. (°C)	Yield (%)
13	**18a**	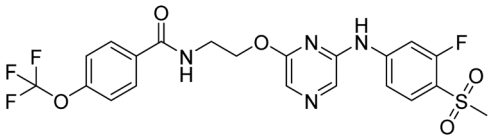	97	66
14	**19a**	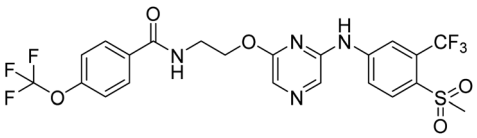	125	59
15	**20a**	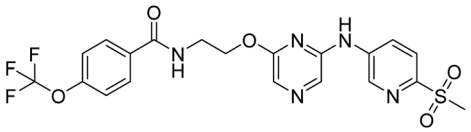	120	53

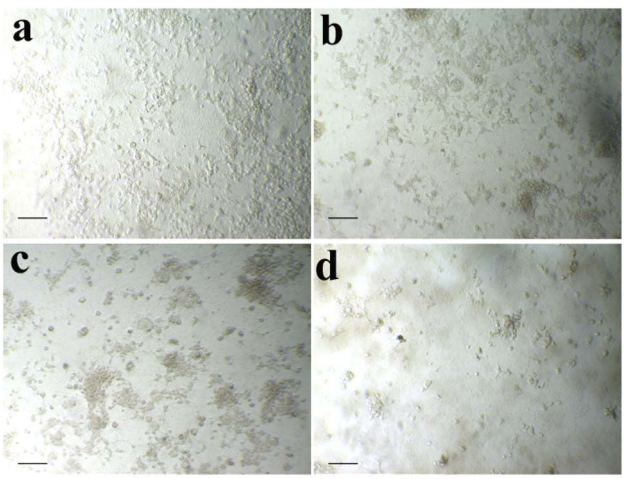

Fig. 2 A549 (lung cancer) cells. Control (a), 10 μg ml^{-1} (b), 25 μg ml^{-1} (c), 50 μg ml^{-1} (d), and scale bars – 50 μm.

culture medium was removed, and 100 μL of the MTT [3-(4,5-dimethylthiozol-2-yl)-3,5-diphenyl tetrazolium bromide] (Hi-Media) solution was added to each well and incubated at 37 °C for 4 h. After removal of the supernatant, 50 μL of DMSO was added to each of the wells and incubated for 10 min to solubilize the formazan crystals. The optical density was measured at 620 nm in an ELISA multi-well plate reader (Thermo Multiskan EX, USA). The OD value was used to calculate the percentage of viability using the following formula.

$$\% \text{ of viability} = \text{OD value of experimental sample/OD value of experimental control} \times 100$$

Fluorescence microscopic analysis of apoptotic cell death

Approximately 1 μL of a dye mixture (100 mg mL^{-1} acridine orange (AO) and 100 mg mL^{-1} ethidium bromide (EtBr) in distilled water) was mixed with 0.9 mL of cell suspension (1 × 10^5 cells per mL) on clean microscope cover slips. The pre-treated cancer cells were collected, washed with phosphate-buffered saline (PBS) (pH 7.2), and stained with 10 μL of AO/EtBr. After incubation for 2 min, the cells were washed twice with PBS (5 min each) and visualized under a fluorescence microscope (Nikon Eclipse, Inc., Japan) at 20× magnification with an excitation filter at 580 nm.[29–32]

Cytotoxic assay. An analysis of the effect of the extract on the cell response of the Human lung cancer cells by using the MTT assay. Fig. 2 shows the *in vitro* cytotoxicity activity of the

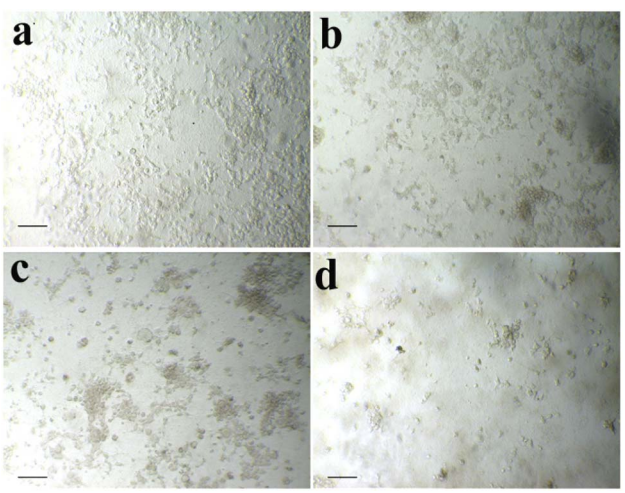

Fig. 3 Morphological changes were observed in A549 cells after treatment with the synthesized compounds at various concentrations.

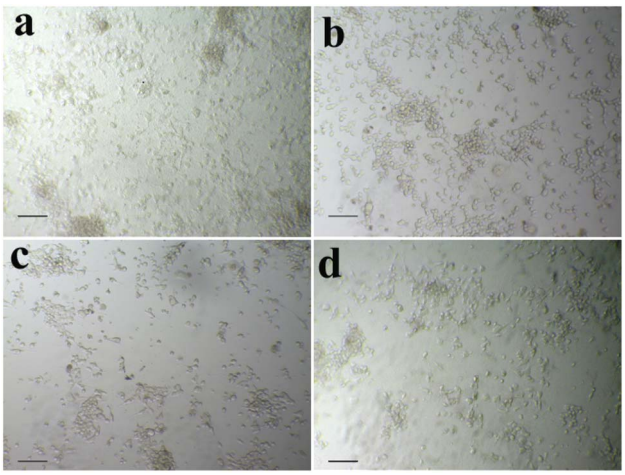

Fig. 4 Morphological changes observed in A549 cells exposed to the synthesized compounds at various concentrations compared to the control.

extract (up to 100 μg ml^{-1} concentrations) against selected lung cancer cells. The experimental results demonstrate that the extract inhibited cell proliferation dose-dependently. From Fig. 2, the IC_{50} values of a sample against cancer cells were calculated, and it was found to be 19 and 17 μg ml^{-1} CPd12 and CPd13 13 respectively. It can be noticed from the results that the observed IC_{50} values of the material are low and significantly inhibit the proliferation of Human cancer cells.

Cell morphology analysis. The morphological changes of selected cancer cells in the absence and presence of samples at various concentrations are shown in Fig. 3 and 4. It could be observed from Fig. 3 and 4, control cells showed no remarkable changes in their morphology. However, in the presence of samples, the cells show improved cell shrinkage and membrane blebbing, and floating cells are formed in a dose-dependent manner. It is well accepted that cytological investigations elucidate the antiproliferative effect mediated through membrane blebbing, membrane instability, and disturbing the cytoskeleton of the cells by the samples.

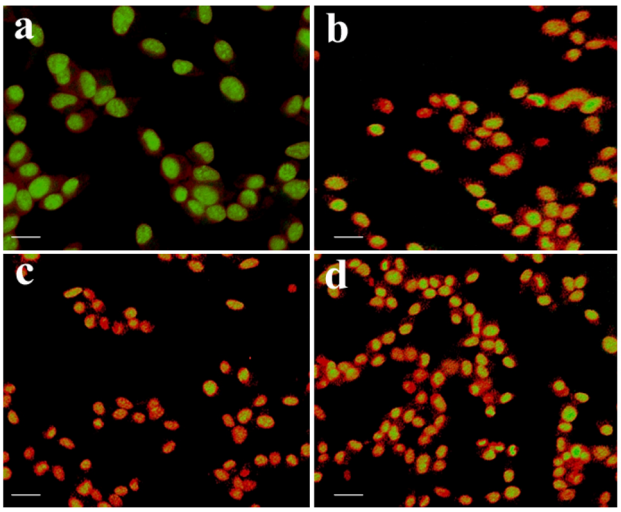

Fig. 5 Fluorescence microscopy images of A549 cancer cells showing morphological changes in the absence (control) and presence of test samples.

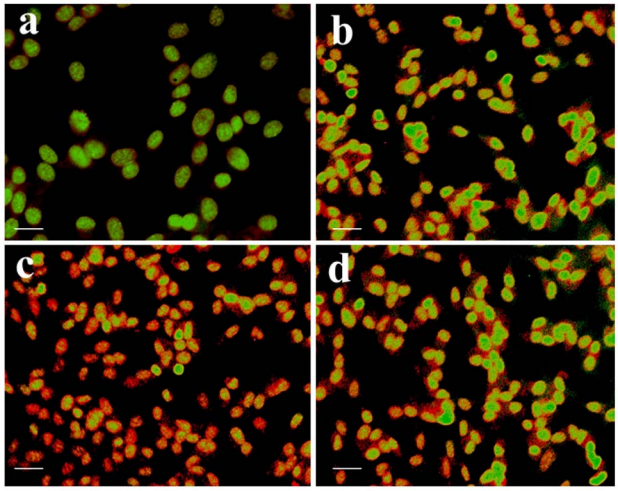

Fig. 6 Control (a), 10 μg ml^{-1} (b), 25 μg ml^{-1} (c), 50 μg ml^{-1} (d), and scale bars – 50 μm.

Table 2 Anticancer activity data of the synthesized 2,6-disubstituted pyrazine scaffolds (μg mL^{-1})[a]

Sample	A549 cells (IC_{50})
Compound **12a**	19 ± 0.5
Compound **13a**	17 ± 0.5
Doxorubicin	16 ± 1.3

[a] IC_{50} – values of respective compounds (at 24 h) standard used: doxorubicin.

Acridine orange/ethidium bromide (AO/EtBr) staining method

In order to study the effect of apoptogenic activity of the material on cancer cells, we conducted the fluorescence microscopic analysis. Fluorescence microscopy images of A549 cancer cells in the absence of samples (Control) and in the presence of samples are shown in Fig. 5. Fig. 5(a) shows that the untreated Lung cancer cells (control) did not show any significant adverse effect compared to the sample treated cells (Fig. 5(b–d)). From Fig. 5(b–d), it can be observed that with the addition of the sample to the A549 cells (Fig. 6), the green color of the cells is transformed into orange/red color cells, which is due to the induction of apoptosis and the nuclear condensation effect on the cells.[33–35]

This choice from the literature to examine the binding mode conformation structure that contributes to the interrelations

Table 3 Antibacterial zone of inhibition of synthesized benzamide derivatives (6a–20a)

		E. coli			*S. aureus*		
S. No.	Compounds	50 (μg ml^{-1})	100 (μg ml^{-1})	150 (μg ml^{-1})	50 (μg ml^{-1})	100 (μg ml^{-1})	150 (μg ml^{-1})
1	**6a**	1.6	2.2	2.4	1.7	1.8	2.1
2	**7a**	1.6	2.1	2.3	1.4	2.0	2.2
3	**8a**	1.5	1.9	2.2	1.6	1.9	2.2
4	**9a**	1.3	1.8	2.1	1.5	1.9	2.2
5	**10a**	1.6	1.8	2.0	1.7	1.8	2.3
6	**11a**	1.7	1.9	2.2	1.8	1.9	2.2
7	**12a**	**1.9**	**2.3**	**2.9**	**1.8**	**2.5**	**3.0**
8	**13a**	1.7	2.2	2.7	1.8	2.1	2.8
9	**14a**	1.6	1.9	2.1	1.5	1.9	2.0
10	**15a**	1.5	1.8	2.2	1.4	1.8	2.0
11	**16a**	1.5	1.8	2.2	1.4	1.8	2.0
12	**17a**	1.3	1.8	2.0	1.8	2.0	2.0
13	**18a**	1.7	2.2	2.2	1.8	2.0	2.0
14	**19a**	1.7	2.2	2.3	1.7	1.9	1.9
15	**20a**	1.6	1.7	1.9	1.8	1.9	2.4
16	Ciprofloxacin	2.0	2.5	3.0	2.0	2.5	3.0

between synthesized compounds and the protein. The best fitted poses, binding energy scores, and a list of hydrogen bonds were determined. From the docking studies, it was predicted that few compounds would have strong interactions against the active site of the bound protein. The rank of potent binding score compounds are: comp. **20** > comp. **12** > comp. **11** > comp. **15** > comp. **19** = −6.8 > −6.7 > −6.5 > −6.4 > −6.2 kcal mol^{-1}. Remaining compounds binding affinities showed good to moderate.[36] Its promising binding affinity suggests potential as an antimicrobial agent. The compounds **12a** and **13a** showed excellent anticancer activity results, which are summarized in Table 2.

$$\text{Formula : } \%\text{ of viability} = \frac{\text{OD value of an experimental sample}}{\text{OD value of experimental control}} \times 100$$

Statistics. All the *in vitro* experiments were done in triplicate and repeated at least three times. The statistical software SPSS version 17.0 was used for the analysis. P value < 0.01 was considered significant.

Antibacterial activity. The antibacterial susceptibility of prepared compounds against Gram-positive and Gram-negative bacterial strains was assessed. *S. aureus* and *E. coli* were evaluated by the disk diffusion/Kirby–Bauer method.[37–41] Briefly, a 100 μL sample of freshly grown bacterial suspension (~10^4 and ~10^6 CFU per mL of *S. aureus* and *E. coli*, respectively, cultured in LB medium) was spread onto nutrient agar plates. Small sterile paper disks of uniform size (10 mm) were impregnated with as-prepared compounds and colloidal samples and then placed on the nutrient agar plates. A disk impregnated with ciprofloxacin was also placed on nutrient agar for positive control, and PBS acted as a negative control, respectively. Plates were then incubated at 37 °C for 24 h. The resulting bacterial colonies' distance inhibition zones around the disks were then recorded.

The antibacterial zone inhibition (mm) of samples against pathogenic microorganisms is given in Table 3. The results revealed that most tested compounds **(6a–20a)** showed moderate to good inhibitory activity against all the strains. All the synthesized compounds (**6a–20a**) showed very good activity.

Molecular docking studies. For affected identification and result enhancement, analytical techniques that "dock" organic compounds into the structures of molecular targets and "score" their potential in pertaining to binding sites are widely applied.[42] The Chem Draw Ultra 15.0 was used to create the structural model, which was then saved as a PDBQT file for Discovery Studio 2021 to display.[43] Using the corresponding 3D structure and the default MOE energy reduction method parameters (gradient: 0.05, Force Field: MMFF94X), the energies of the observed molecule were decreased. The obtained model was then used in the MOE's "Systematic Conformational Search." Selected protein (PDBID: ICEI) crystal structures were obtained *via* the Protein Data Bank (**http://www.rcsb.org/pdb**). The proteins were fixed in a variety of ways before docking, such as by deleting solvent molecules and co-ligands, introducing hydrogen's, altering the chain, and selecting active sites. The novel synthesized modeled compounds (**6a** to **20a**) docked with the active site of the antibacterial protein residual (PDBID: 1CEI). The modeled three-dimensional (3-D) and two-dimensional (2-D) compounds and their distances between atoms (Å), binding interactions, and binding energies are shown in Tables 4 and 5.

Conclusion

In summary, a new series of biologically potent *N*-(2-(6-substituted-1*H*-pyrazin-2-yloxy)ethyl)-4-(trifluoromethoxy)benzamide derivatives was successfully synthesized and characterized by ^{1}H NMR, ^{13}C NMR, and mass spectrometry. The

Table 4 The molecular docking interaction of compounds with the antibacterial protein (PDBID: 1CEI)

S. No.	Compounds	Interaction residues (PDBID: 1CI)		Distances (Å)	H-interactions involved	Binging energy (kcal mol^{-1})
		Ligand	Protein			
1	**6a**	NH	O-GLU: A14	3.01	2	−5.9
		O	HN-LEU: A3	2.26		
2	**7a**	O	HN-LYS: A70	2.33	3	−6.5
		N	HN-LYS: A70	2.43		
		O	HN-ASP: A62	2.05		
3	**8a**	NH	O-GLU: A21	2.34	2	−6.2
		O	HN-GLN: A17	2.34		
4	**9a**	NH	O-ASP: A35	2.46	2	−6.4
		O	HO-THR: A51	2.76		
5	**10a**	N	HN-LYS: A81	2.36	1	−6.1
6	**11a**	O	HN-LEU; A3	2.42	2	−6.5
		F	HN-LEU; A3	2.70		
7	**12a**	F	HN-LEU: A3	2.84	4	−6.7
		NH	O-GLN: A17	2.15		
		N	HO-THR: A11	2.21		
		O	HN-LYS:85	1.94		
8	**13a**	NH	O-GLU: A21	2.43	3	−5.7
		NH	O-GLN: A17	3.08		
		F	HN-LEU: A3	2.08		
9	**14a**	NH	O-ASN: A60	2.31	3	−5.4
		O	HO-SER: A58	2.20		
		O	HN-LYS: A70	3.30		
10	**15a**	F	HN-LYS: A70	2.93	3	−6.4
		F	HN-LYS: A70	2.75		
		N	HN-HYS: A47	2.49		
11	**16a**	N	HO-SER: A58	2.30	3	−6.0
		N	HN-ASN: A60	2.38		
		F	O-HNASN: A79	2.95		
12	**17a**	O	HN-GLY: A17	2.80	4	−5.5
		NH	O-GLY: A17	2.65		
		NH	O-GLU: A21	2.37		
		F	HN-LEU: A3	2.42		
13	**18a**	N	HN-LEU: A3	3.02	3	−5.4
		NH	O-GLU:21	2.31		
		O	HN-GLN: A17	2.38		
14	**19a**	O	HN-LYS: A70	2.47	3	−6.2
		F	O-LYS: A70	2.78		
		O	HN-HYS: A47	2.18		
15	**20a**	F	HN-PHE: A84	2.53	5	−6.5
		F	HN-PHE: A84	2.57		
		O	HN-LYS: A73	2.32		
		NH	O-GLU: A66	2.45		
		O	HN-GLY: A87	2.33		

biological screening highlighted the dual therapeutic potential of these compounds, with **12a** and **13a** exhibiting notable antibacterial activity against *Staphylococcus aureus* and *Escherichia coli*. Furthermore, these lead compounds demonstrated significant anticancer activity against the A549 lung cancer cell line, with IC_{50} values of 19 ± 0.50 μM and 17 ± 0.50 μM, respectively. Molecular docking studies supported the experimental findings, indicating strong intercalative interactions between the synthesized molecules and their respective target proteins. These results underscore the potential of **12a** and **13a** as promising scaffolds.

Experimental section

All the chemicals used in the present investigation were purchased from Sigma-Aldrich Chemical Company, India. Melting points were determined on a Cintex melting point apparatus and are uncorrected. The purity of the compounds was monitored by TLC on silica gel-G plates (Merk, 60F 254), visualized with ultraviolet light. IR spectra (KBr) were recorded on a PerkinElmer BX series FT-IR spectrophotometer, and 1H and ^{13}C-NMR spectra on a Varian Gemini 400 MHz spectrometer (Chemical shifts in δ ppm) using TMS as internal

Table 5 3D and 2D molecular docking poses interactions between compounds with the active sites of the bacterial protein (PDBID: 1CEI)

S. No	Compounds	3D structure of a molecule interaction with an enzyme	2D structure of a molecule interaction with protein
6	**11a**	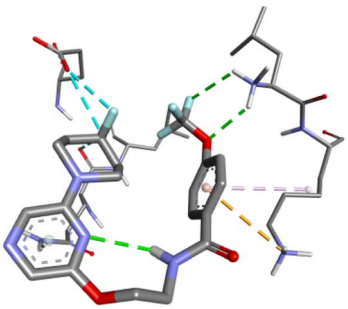	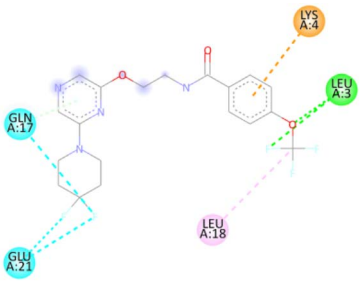
7	**12a**	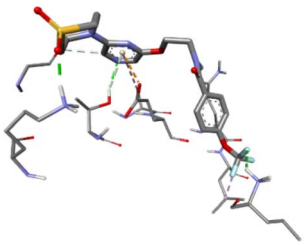	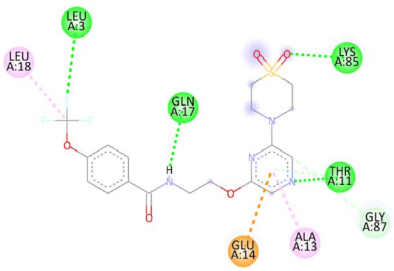
10	**15a**	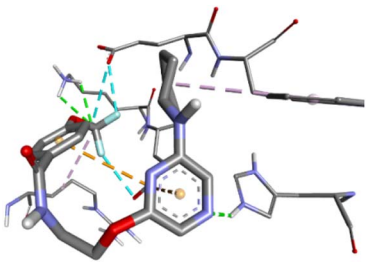	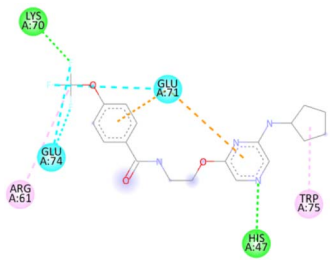
14	**19a**	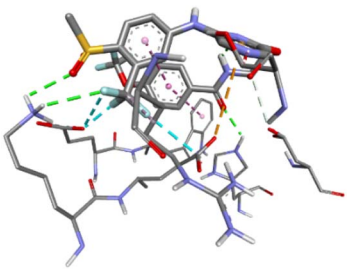	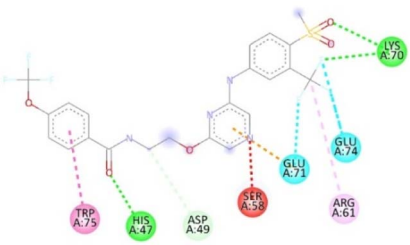
15	**20a**	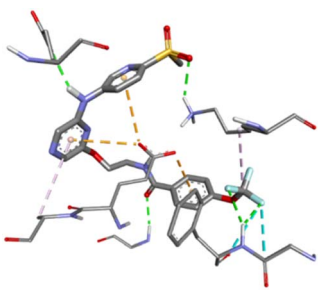	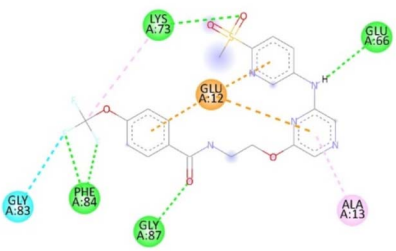

standard. Mass spectra were recorded using the electron spray ionization technique on the LCMS-2010A mass spectrometer at 70 eV.

General procedure for the construction of *N*-(2-hydroxyethyl)-4-(trifluoromethoxy)benzamide (3)

To a stirred solution of 4-(trifluoromethoxy)benzoic acid (5 g, 24.26 mmol; 1 eq.) in THF (100 mL) was added 2-aminoethan-1-

ol (1.63 g, 26.68 mmol; 1.1 eq.) followed by DIPEA (12.68 mL, 72.77 mmol; 3 eq.), HOBt (4.92 g, 36.39 mmol; 1.5 eq.) and EDC. HCl (6.98 g, 36.39 mmol; 1.5 eq.) was added at 0 °C and stirred for 12 h at 25 °C. After completion of the reaction, the reaction mixture was diluted with EtOAc (200 mL) and washed with water (200 mL) and brine solution (100 mL). The separated organic layer was concentrated and purified by column chromatography using a silica gel column to yield *N*-(2-hydroxyethyl)-4-(trifluoromethoxy)benzamide (5.1 g, 20.46 mmol; 84.83% Yield), white solid. ^{1}H NMR (400 MHz, DMSO-d_6): δ 8.55 (t, J = 5.20 Hz, 1H), 7.98 (dd, J = 2.80, 5.80 Hz, 2H), 7.46 (d, J = 8.00 Hz, 2H), 4.73 (t, J = 5.60 Hz, 1H), 3.54–3.49 (m, 2H), 3.36–3.31 (m, 2H). ^{13}C NMR (101 MHz, DMSO-d_6): δ 165.54, 150.63, 134.15, 129.98, 121.72, 121.01, 119.16, 60.11, 42.72. ^{19}F NMR (377 MHz, DMSO-d6): δ −56.69. LCMS: m/z: 250.0 $(M + H)^+$.

General procedure for the synthesis of *N*-(2-((6-chloropyrazin-2-yl)oxy)ethyl)-4-(trifluoromethoxy)benzamide (5)

To a stirred solution of *N*-(2-hydroxyethyl)-4-(trifluoromethoxy) benzamide (5 g, 20.07 mmol; 1 eq.) in THF (80 mL) was added 2,6-dichloropyrazine (2.99 g, 20.07 mmol; 1 eq.) followed by potassium *tert*-butoxide (2.48 g, 22.07 mmol; 1.1 eq.) in THF (20 mL) at 0 °C and stirred for 2 h at 25 °C. After completion of the reaction, the reaction mixture was diluted with EtOAc (200 mL) and washed with water (100 mL) and brine solution (100 mL). The separated organic layer was concentrated and purified by column chromatography using a silica gel column to yield *N*-(2-((6-chloropyrazin-2-yl)oxy)ethyl)-4-(trifluoromethoxy)benzamide (6.2 g, 17.14 mmol; 84% Yield), white solid. 1H-NMR (400 MHz, DMSO-d_6): δ 8.80 (s, 1H), 8.33 (d, J = 6.40 Hz, 2H), 7.97 (d, J = 8.40 Hz, 2H), 7.47 (d, J = 8.40 Hz, 2H), 4.48 (t, 2H), 3.69 (m, 2H). ^{13}C NMR (101 MHz, DMSO-d_6): δ 165.79, 159.28, 150.76, 144.65, 135.57, 134.10, 133.75, 130.02, 121.71, 121.08, 119.15, 65.81, 40.62. ^{19}F NMR (377 MHz, DMSO-d_6): −56.69. LCMS: m/z: 362.1 $(M + H)^+$.

General method for the synthesis of *N*-(2-((6-(piperidin-1-yl) pyrazin-2-yl)oxy)ethyl)-4-(trifluoromethoxy)benzamide compounds (6a–13a)

To a stirred solution of *N*-(2-((6-chloropyrazin-2-yl)oxy)ethyl)-4-(trifluoromethoxy)benzamide (1 eq.) in DMSO (w/v 20%) was added 2°-amines (**6a** to **13a**) (2 eq.) at room temperature and stirred for 12 h at 80 °C. After completion of the reaction, the reaction mixture was diluted with EtOAc and washed with water and brine solution. The separated organic layer was concentrated and purified by column chromatography using a silica gel column to yield the desired compounds **6a** to **13a**.

***N*-(2-((6-(azetidin-1-yl)pyrazin-2-yl)oxy)ethyl)-4-(trifluoromethoxy)benzamide (6a).** ^{1}H NMR (400 MHz, DMSO-d_6): δ 8.80 (t, J = 5.60 Hz, 1H), 7.98–7.95 (m, 2H), 7.47–7.44 (m, 3H), 7.34 (s, 1H), 4.37 (t, J = 5.60 Hz, 2H), 3.98 (t, J = 7.60 Hz, 4H), 3.66–3.61 (m, 2H), 2.37–2.30 (m, 2H). ^{13}C NMR (101 MHz, DMSO-d_6): δ 165.69, 158.93, 154.85, 150.74, 133.83, 130.011, 121.701, 121.07, 120.79, 120.12, 119.15, 64.10, 50.94, 17.02. LCMS: m/z: 427.0 $(M + H)^+$.

***N*-(2-((6-(pyrrolidin-1-yl)pyrazin-2-yl)oxy)ethyl)-4-(trifluoromethoxy)benzamide (7a).** ^{1}H NMR (400 MHz, DMSO-d_6): δ 8.79 (t, J = 5.60 Hz, 1H), 7.96–7.94 (m, 2H), 7.47–7.37 (m, 4H), 4.41 (t, J = 5.60 Hz, 2H), 3.66–3.62 (m, 2H), 3.39–3.34 (m, 4H), 1.92–1.89 (m, 4H). ^{13}C NMR (101 MHz, DMSO-d_6): δ 165.70, 158.70, 151.55, 150.71, 133.85, 129.99, 124.26, 121.70, 121.44, 121.05, 119.15, 118.49, 116.6, 63.84, 46.44, 25.24. LCMS: m/z: 441.0 $(M + H)^+$.

***N*-(2-((6-(piperidin-1-yl)pyrazin-2-yl)oxy)ethyl)-4-(trifluoromethoxy)benzamide (8a).** ^{1}H NMR (400 MHz, DMSO-d_6): δ 8.79 (t, J = 5.60 Hz, 1H), 7.96 (d, J = 8.40 Hz, 2H), 7.78 (s, 1H), 7.46 (d, J = 8.40 Hz, 2H), 7.40 (s, 1H), 4.38 (t, J = 5.60 Hz, 2H), 3.64 (q, J = 5.60 Hz, 2H), 3.53–3.50 (m, 4H), 1.59–1.52 (m, 6H). ^{13}C NMR (101 MHz, DMSO-d_6):δ 165.70, 158.24, 153.32, 150.72, 133.84, 130.02, 121.84, 121.07, 119.54, 63.93, 45.45, 25.29, 24.52. LCMS: m/z: 411.2 $(M + H)^+$.

***N*-(2-((6-morpholinopyrazin-2-yl)oxy)ethyl)-4-(trifluoromethoxy)benzamide (9a).** ^{1}H NMR (400 MHz, DMSO-d_6):δ 8.79 (t, J = 5.60 Hz, 1H), 7.97–7.93 (m, 2H), 7.79 (s, 1H), 7.51 (s, 1H), 7.46 (d, J = 8.00 Hz, 2H), 4.42–4.39 (m, 2H), 3.67–3.63 (m, 6H), 3.48–3.45 (m, 4H), ^{13}C NMR (101 MHz, DMSO-d_6): δ 165.71, 158.23, 153.40, 150.3, 133.83, 130.01, 121.81, 121.70, 121.08, 119.15 66.16, 64.02, 44.81. LCMS: m/z: 413.0 $(M + H)^+$.

***N*-(2-((6-(4-cyanopiperidin-1-yl)pyrazin-2-yl)oxy)ethyl)-4-(trifluoromethoxy)benzamide (10a).** ^{1}H NMR (400 MHz, DMSO-d_6): δ 8.79 (t, J = 5.60 Hz, 1H), 7.97–7.94 (m, 2H), 7.83 (s, 1H), 7.48–7.45 (m, 3H), 4.39 (t, J = 5.60 Hz, 2H), 3.84–3.79 (m, 2H), 3.67–3.62 (m, 2H), 3.39–3.36 (m, 2H), 3.15–3.10 (m, 1H), 1.95–1.90 (m, 2H), 1.74–1.66 (m, 2H). ^{13}C NMR (101 MHz, DMSO-d_6): 165.72, 158.21, 152.90, 150.74, 133.82, 130.00, 122.46, 122.04, 121.71, 121.05, 120.56, 119.15, 64.03, 43.00, 27.83, 25.88. LCMS: m/z: 436.0 $(M + H)^+$.

***N*-(2-((6-(4,4-difluoropiperidin-1-yl)pyrazin-2-yl)oxy)ethyl)-4-(trifluoromethoxy)benzamide (11a).** ^{1}H NMR (400 MHz, DMSO-d_6): ^{1}H-NMR (400 MHz, DMSO-d6): δ 8.79 (t, J = 5.60 Hz, 1H), 7.96–7.92 (m, 3H), 7.52 (s, 1H), 7.46 (d, J = 8.00 Hz, 2H), 4.41 (t, J = 5.60 Hz, 2H), 3.70–3.62 (m, 6H), 2.03–1.95 (m, 4H). LCMS: m/z: 447.2 $(M + H)^+$.

***N*-(2-((6-(1,1-dioxidothiomorpholino)pyrazin-2-yl)oxy)ethyl)-4-(trifluoromethoxy)benzamide (12a).** ^{1}H NMR (400 MHz, DMSO-d_6): δ 8.80 (t, J = 5.60 Hz, 1H), 7.99–7.95 (m, 3H), 7.58 (s, 1H), 7.47 (d, J = 8.00 Hz, 2H), 4.40 (t, J = 5.60 Hz, 2H), 4.06 (s, 4H), 3.67–3.63 (m, 2H), 3.15 (s, 4H). LCMS: m/z: 461.0 $(M + H)^+$.

***N*-(2-((6-(4-methyl piperazine-1-yl)pyrazin-2-yl)oxy)ethyl)-4-(trifluoromethoxy)benzamide (13a).** ^{1}H NMR (400 MHz, DMSO-d_6): δ 8.79 (t, J = 5.20 Hz, 1H), 7.95 (d, J = 8.80 Hz, 2H), 7.79 (s, 1H), 7.47–7.45 (m, 3H), 4.40 (t, J = 5.60 Hz, 2H), 3.64 (q, J = 5.60 Hz, 2H), 3.49 (t, J = 4.80 Hz, 4H), 2.35 (t, J = 4.80 Hz, 4H), 0.19 (t, J = Hz, 3H). ^{13}C NMR (101 MHz, DMSO-d_6): 165.72, 158.22, 153.31, 150.72, 133.84, 130.01, 121.87, 121.71, 121.06, 120.50, 119.15, 63.97, 54.54, 46.23, 44.40. LCMS: m/z: 426.2 $(M + H)^+$.

General method for synthesis of *N*-(2-((6-(cyclobutylamino) pyrazin-2-yl)oxy)ethyl)-4-(trifluoromethoxy)benzamide derivatives (14a to 16a)

To a stirred solution of *N*-(2-((6-chloropyrazin-2-yl)oxy)ethyl)-4-(trifluoromethoxy)benzamide (1 eq.) in DMSO (w/v 20%) was

added 1°-amines (**14a** to **16a**) (3 eq.) at room temperature and stirred for 12 h at 120 °C. After completion of the reaction, the reaction mixture was diluted with EtOAc and washed with water and brine solution. The separated organic layer was concentrated and purified by column chromatography using a silica gel column to yield the desired compounds **14**, **15**, and **16**.

***N*-(2-((6-(cyclobutylamino)pyrazin-2-yl)oxy)ethyl)-4-(trifluoromethoxy)benzamide (14a).** ^{1}H NMR (400 MHz, DMSO-d_6): δ 8.79 (t, J = 5.60 Hz, 1H), 7.98 (d, J = 8.80 Hz, 2H), 7.47 (d, J = 8.00 Hz, 2H), 7.40 (s, 1H), 7.28 (s, 1H), 7.25 (d, J = 6.80 Hz, 1H), 4.36 (t, J = 5.60 Hz, 2H), 4.24–4.18 (m, 1H), 3.68–3.62 (m, 2H), 2.50–2.28 (m, 2H), 1.92–1.86 (m, 2H), 1.71–1.66 (m, 2H). ^{13}C NMR (101 MHz, DMSO-d_6): 165.71, 159.01, 152.94, 150.72, 133.86, 130.02, 123.16, 121.71, 121.08, 119.16, 118.34, 63.98, 46.16, 30.77, 15.30. LCMS: m/z: 397.2 $(M + H)^+$.

***N*-(2-((6-(cyclopentyl amino)pyrazin-2-yl)oxy)ethyl)-4-(trifluoromethoxy)benzamide (15a).** ^{1}H NMR (400 MHz, DMSO-d_6): δ 8.79 (t, J = 4.80 Hz, 1H), 7.98 (d, J = 8.80 Hz, 2H), 7.47–7.44 (m, 3H), 7.25 (s, 1H), 6.99 (d, J = 6.40 Hz, 1H), 4.37 (t, J = 5.60 Hz, 2H), 4.06–4.01 (m, 1H), 3.66–3.62 (m, 2H), 1.93–1.90 (m, 2H), 1.67–1.62 (m, 2H), 1.59–1.50 (m, 2H), 1.44–1.41 (m, 2H). ^{13}C NMR (101 MHz, DMSO-d_6): 165.69, 159.02, 153.77, 150.72, 133.85, 130.01, 123.69, 121.71, 121.06, 119.16, 117.65, 63.97, 52.33, 32.84, 24.00. LCMS: m/z: 411.2 $(M + H)^+$.

***N*-(2-((6-(cyclohexylamino)pyrazin-2-yl)oxy)ethyl)-4-(trifluoromethoxy)benzamide (16a).** ^{1}H NMR (400 MHz, DMSO-d_6):δ 8.79 (t, J = 5.20 Hz, 1H), 7.98–7.95 (m, 2H), 7.47–7.45 (m, 3H), 7.23 (s, 1H), 6.86 (d, J = 7.60 Hz, 1H), 4.37–4.34 (m, 2H), 3.66–3.57 (m, 3H), 3.66–3.57 (m, 2H), 1.72–1.68 (m, 2H), 1.59–1.56 (m, 1H), 1.36–1.20 (m, 6H); LCMS: m/z: 425.1 $(M + H)^+$.

General method for the construction of *N*-(2-((6-((2-fluoro-4-(methyl sulfonyl)phenyl)amino)pyrazin-2-yl)oxy)ethyl)-4-(trifluoromethoxy)benzamide derivatives (17a–20a)

To a stirred solution of *N*-(2-((6-chloropyrazin-2-yl)oxy)ethyl)-4-(trifluoromethoxy)benzamide (1 eq.) in 1,4-dioxane (w/v 20%) was added amine (**17a–20a**), Cs_2CO_3 (2.5 eq.) and degassed with argon for 2 min and to this resulting reaction mixture was added Brett-Phos Pd G_3 (0.05 eq.) at room temperature and stirred for 12 h at 110 °C. After completion of the reaction, the reaction mixture was diluted with EtOAc and washed with water and brine solution. The separated organic layer was concentrated and purified by column chromatography using a silica-gel column to yield the desired compounds **17a** to **20a**.

***N*-(2-((6-((2-fluoro-4-(methyl sulfonyl)phenyl)amino)pyrazin-2-yl)oxy)ethyl)-4-(trifluoromethoxy)benzamide (17a).** ^{1}H NMR (400 MHz, DMSO-d_6):δ 9.66 (s, 1H), 8.81 (t, J = 5.60 Hz, 1H), 8.53 (t, J = 8.00 Hz, 1H), 8.12 (s, 1H), 7.99–7.91 (m, 2H), 7.81–7.66 (m, 3H), 7.45 (d, J = 8.00 Hz, 2H), 4.48 (t, J = 5.20 Hz, 2H), 3.72–3.68 (m, 2H), 3.23 (s, 3H). LCMS: m/z: 515.0 $(M + H)^+$.

***N*-(2-((6-((3-fluoro-4-(methyl sulfonyl)phenyl)amino)pyrazin-2-yl)oxy)ethyl)-4-(trifluoromethoxy)benzamide (18a).** ^{1}H NMR (400 MHz, DMSO-d_6): δ 10.23 (s, 1H), 8.83 (t, J = 5.20 Hz, 1H), 7.97–7.95 (m, 1H), 7.89 (s, 1H), 7.80–7.76 (m, 3H), 7.57–7.54 (m, 1H), 7.46 (d, J = 8.00 Hz, 2H), 4.51 (t, J = 5.20 Hz, 2H), 3.75–3.71 (m, 2H), 3.26 (s, 3H). LCMS: m/z: 515.0 $(M + H)^+$.

***N*-(2-((6-((4-(methyl sulfonyl)-3-(trifluoromethyl)phenyl)amino)pyrazin-2-yl)oxy)ethyl)-4-(trifluoromethoxy)benzamide (19a).** ^{1}H NMR (400 MHz, DMSO-d_6):δ 10.38 (s, 1H), 8.83 (t, J = 5.20 Hz, 1H), 8.39 (d, J = 2.00 Hz, 1H), 8.18–8.15 (m, 1H), 8.09–8.06 (m, 1H), 7.99–7.94 (m, 2H), 7.94 (s, 1H), 7.79 (s, 1H), 7.46–7.44 (m, 2H), 4.50 (t, J = 5.60 Hz, 2H), 3.74–0.70 (m, 2H), 3.23 (s, 3H). LCMS: m/z: 565.0 $(M + H)^+$.

***N*-(2-((6-((6-(methyl sulfonyl)pyridin-3-yl)amino)pyrazin-2-yl)oxy)ethyl)-4-(trifluoromethoxy)benzamide (20a).** ^{1}H NMR (400 MHz, DMSO-d_6): δ 10.24 (s, 1H), 8.92 (d, J = 2.40 Hz, 2H), 8.83 (t, J = 5.60 Hz, 1H), 8.43–8.41 (m, 1H), 7.97–7.91 (m, 5H), 7.77 (s, 1H), 7.45 (d, J = 8.00 Hz, 2H), 4.52 (t, J = 5.60 Hz, 2H), 3.74–3.70 (m, 2H), 3.22 (s, 3H). LCMS: m/z: 498.0 $(M + H)^+$.

Data availability

The data supporting this article have been included as part of the ESI.†

Conflicts of interest

There are no conflicts to declare.

Acknowledgements

The authors are grateful to acknowledge financial support from Syngeneic International Ltd, under which this research was pursued. We are thankful to Syngene International Ltd, Hyderabad, for providing spectral data and the Department of Biochemistry, Bharathiar University, Coimbatore, for their valuable contribution to doing biological studies.

References

1 D. Choudhary, S. Garg, M. Kaur, H. Singh Sohal, D. Singh Malhi, L. Kaur, M. Verma, A. Sharma and V. Mutreja, *Polycyclic Aromat. Compd.*, 2023, **43**(5), 4512–4578.
2 A. Climova, E. Pivovarova, B. Rogalewicz, A. Raducka, M. Szczesio, I. Korona-Głowniak, A. Korga-Plewko, M. Iwan, K. Gobis and A. Czylkowska, *Molecules*, 2022, **27**(11), 3467.
3 A. Hameed, S. T. Zehra, S. J. A. Shah, K. M. Khan, R. D. Alharthy, N. Furtmann, J. Bajorath, M. N. Tahir and J. Iqbal, *Chem. Biol. Drug Des.*, 2015, **86**, 1115–1120.
4 G.-Q. Chen, H.-Y. Guo, Z.-S. Quan, Q.-K. Shen, X. Li and T. Luan, *Molecules*, 2023, **28**(21), 7440.
5 H. Wen, W. Dai, H. Huang, S.-L. Liu, J. Liu, Le-J. Huang, X.-H. Huang, J.-L. Zeng, Z.-W. Gan, Z.-Y. Zhang and J.-X. Lan, *Eur. J. Med. Chem.*, 2023, **258**, 115544.
6 L. Peng-Cheng, H.-Q. Li, J. Sun, Z. Yang and H.-L. Zhu, *Bioorg. Med. Chem.*, 2010, **18**(13), 4606–4614.
7 M. L. N. Dubuisson and M.-B. Rees, *Med. Chem.*, 2004, **4**(15), 421–435.
8 K. Singh*, J. K. Gupta, K. Shah, S. Saha, M. Arockia Babu, S. Kumar and M. Agrawal, *Curr. Org. Chem.*, 2024, **28**(3), 176–184.
9 H.-M. Wu, K. Zhou, T. Wu and Y.-G. Cao, *Chem. Biol. Drug Des.*, 2016, **88**(3), 411–421.

10 K. Zurbonsen, A. Michel, P.-A. Bonnet, L. Gannoun-Zaki, M.-N. Mathieu and C. Chevillard, *Eur. J. Pharmacol.*, 1997, **320**(2–3), 215–221.
11 J. Hu, S. Chen, R. Mao, C. Liao, H. Yang and J. Zhao, *J. Inorg. Biochem.*, 2018, **186**, 246–256.
12 R. Sahu, K. Shah, Y. Gautam and K. Sahu, *Curr. Org. Chem.*, 2023, **27**(23), 821–843.
13 H. Zhang, Y. Wang, P. Zhu, J. Liu, S. Xu, H. Yao, J. Jiang, W. Ye, X. Wu and J. Xu, *Eur. J. Med. Chem.*, 2015, **97**, 235–244.
14 O. Argyros, N. Lougiakis, E. Kouvari, A. Papafotika, C. P. Raptopoulou, V. Psycharis, S. Christoforidis, N. Pouli, P. Marakos and C. Tamvakopoulos, *Eur. J. Med. Chem.*, 2017, **126**, 954–968.
15 J.-H. Zhang, C.-D. Fan, Z. Bao-Xiang, D.-S. Shin, W.-L. Dong, Y.-S. Xie and J.-Y. Miao, *Bioorg. Med. Chem.*, 2008, **16**(24), 10165–10171.
16 S. Akhlaghi, A. Mostoufi, H. Kalantar and M. Fereidoonnezhad, *Med. Chem. Res.*, 2022, **31**, 580–593.
17 Zi-Q. Liu, Q. Zhang, Yu-L. Liu, X.-Q. Yu, R.-H. Chui, L.-L. Zhang, B. Zhao and L.-Y. Ma, *Bioorg. Med. Chem.*, 2024, **111**, 117847.
18 M. Tan Uygun, K. Amudi, İ. D. Turaçlı and N. Menges, *Mol. Diversity*, 2022, **26**, 113–124.
19 P. Parsonidis, M. Shaik, A. Panagiota Serafeim, I. Vlachou, V. Daikopoulou and I. Papasotiriou, *Molecules*, 2019, **24**(23), 4389.
20 E. S. Tantawy, A. M. Amer, E. K. Mohamed, M. M. Abd Alla and M. S. Nafie, *J. Mol. Struct.*, 2020, **1210**, 128013.
21 J. Akhtar, A. Ahmed Khan, Z. Ali, R. Haider and M. Shahar Yar, *Eur. J. Med. Chem.*, 2017, **125**, 143–189.
22 M. Youssef Jaballah, R. Taha Serya and K. Abouzid, *Drug Res.*, 2017, **67**(03), 138–148.
23 K. Fang, X.-H. Zhang, Y.-T. Han, G.-R. Wu, De-S. Cai, N.-N. Xue, W.-B. Guo, Yu-Q. Yang, M. Chen, X.-Y. Zhang, H. Wang, T. Ma and P.-L. Wang, *Int. J. Mol. Sci.*, 2018, **19**(10), 2994.
24 A. Alsfouk, *Future Med. Chem.*, 2024, **16**(18), 1899–1921.
25 Y.-D. Gong, Mi-S. Dong, S.-B. Lee, N. Kim, Mi-S. Bae and N.-S. Kang, *Bioorg. Med. Chem.*, 2011, **19**(18), 5639–5647.
26 K. Fang, X.-H. Zhang, Y.-T. Han, G.-R. Wu, De-S. Cai, N.-N. Xue, W.-B. Guo, Yu-Q. Yang, M. Chen, X.-Y. Zhang, H. Wang, T. Ma, P.-L. Wang and H.-M. Lei, *Int. J. Mol. Sci.*, 2018, **19**(10), 2994.
27 F. A. López-Huerta, M. Teresa Ramírez-Apan, C. A. Méndez-Cuesta, A. Nieto-Camacho, S. Hernández-Ortega, E. K. P. Almeida-Aguirre, M. A. Cerbón and G. Delgado, *Bioorg. Chem.*, 2022, **125**, 105924.
28 P. Bera, A. Aher, P. Brandao, S. K. Manna, I. Bhattacharyya, G. Mondal, A. Jana and A. S. Pulakesh Bera, *New J. Chem.*, 2021, **45**, 11999–12015.
29 X. De Wang, T. Li, Y. Li, W. Hui Yuan and Y. Q. Zhao, *Eur. J. Pharmacol.*, 2020, **881**, 173211.
30 S. Rostampour, F. Eslami, E. Babaei, H. Mostafavi and M. Mahdavi, *Anti-Cancer Agents Med. Chem.*, 2024, **24**(10), 203–212.
31 J. Hodoň, I. Frydrych, Z. Trhlíková, J. Pokorný, L. Borková, S. Benická, M. Vlk, B. Lišková, A. Kubíčková, M. Medvedíková, M. Pisár, J. Šarek, V. Das, A. Ligasová, K. Koberna, P. Džubák, M. Hajdúch and M. Urban, *Eur. J. Med. Chem.*, 2022, **243**, 114777.
32 K. Zurbonsen, A. Michel, P. A. Bonnet, M. N. Mathieu and C. Chevillard, *Gen. Pharmacol.*, 1999, **32**(1), 135–141.
33 R. Khanam, R. Kumar, I. Iqbal Hejazi, S. Shahabuddin, R. Meena, V. Jayant, P. Kumar, A. R. Bhat and F. Athar, *Apoptosis*, 2018, **23**, 113–131.
34 S. Behzad, E. Karim, M. Mosaddegh and H. Ali, *Iran. J. Pharm. Res.*, 2016, **15**(1), 311–322.
35 R. Prabaharan, R. Ramesh, S. Kamatchi Thangavel and J. G. Małecki, *ACS Omega*, 2023, **8**(13), 12584–12591.
36 O. Trott and A. J. Olson, *J. Comput. Chem.*, 2009, 455–461.
37 S. K. Wahan, S. Sharma and P. A. Chawla, *Med. Chem.*, 2023, **23**(19), 700–718.
38 N. W. Hassan, M. N. Saudi, Y. S. Abdel-Ghany, A. Ismail, P. A. Elzahhar, D. Sriram, R. Nassra, M. M. Abdel-Aziz and S. A. El-Hawash, *Bioorg. Chem.*, 2020, **96**, 103610.
39 L. Semelkova, K. Konecna, P. Paterova, V. Kubicek, J. Kunes, L. Novakova, J. Marek, L. Naesens, M. Pesko, K. Kralova, M. Dolezal and J. Zitko, *Molecules*, 2015, **20**(5), 8687–8711.
40 S. kumar, P. Dinesha, D. Udayakumar, V. Prakash Shetty and V. Kumar Deekshit, *J. Mol. Struct.*, 2024, **1304**, 137657.
41 A. A. Siddiki, S. Parmar, H. K. Chaudhari, S. SP Yadav and R. S. Chauhan, *ChemistrySelect*, 2024, **9**(36), e202402487.
42 M. M. El-Zahed, M. A. Diab, A. Z. El-Sonbati, S. G. Nozha, H. R. Issa, M. A. El-Mogazy and Sh. M. Morgan, *Mater. Sci. Eng., B*, 2024, **299**, 116998.
43 T. Bhat and T. J. Richmond, *Discovery Studio Visualizer software, Dassault Systèmes BIOVIA, Version 9*, 2021.